PCCP

Rapid acquisition of data dense solid-state CPMG NMR spectral sets using multi-dimensional statistical analysis

Journal:	*Physical Chemistry Chemical Physics*
Manuscript ID	CP-ART-04-2018-002382.R1
Article Type:	Paper
Date Submitted by the Author:	31-May-2018
Complete List of Authors:	Mason, Harris; Lawrence Livermore National Laboratory, Uribe, Eva; Sandia National Laboratories California, Systems and Research Analysis Group Shusterman, Jennifer; Hunter College, Chemistry

SCHOLARONE™
Manuscripts

Physical Chemistry Chemical Physics

ARTICLE

Rapid acquisition of data dense solid-state CPMG NMR spectral sets using multi-dimensional statistical analysis

Received 00th January 20xx,
Accepted 00th January 20xx

DOI: 10.1039/x0xx00000x

www.rsc.org/

H. E. Mason,[a] E. C. Uribe[b] and J. A. Shusterman[c]

The development of multi-dimensional statistical methods have been demonstrated on variable contact time (VCT) $^{29}Si\{^{1}H\}$ cross-polarization magic angle spinning (CP/MAS) data sets collected with Carr-Purcell-Meiboom-Gill (CPMG) type acquisition. These methods utalize a transformation of the collected 2D VCT data set into a 3D data set and use tensor-rank decomposition to extract the spectral components that are varying as a function of transverse relaxation time (T_2) and CP contact time. The result is a data dense spectral set that can be used to reconstruct CP/MAS spectra at any contact time with high signal to noise and with excellent agreement to $^{29}Si\{^{1}H\}$ CP/MAS spectra collected with conventional acquisition. These CPMG data can be collected in a fraction of the time that would be required to collect a conventional VCT data set. We demonstrate the method on samples of functionalized mesoporous silica materials and show that the method can provide valuable surface specific information about their functional chemistry.

1. Introduction

Solid-state NMR holds exciting potential for structural and chemical determinations in a wide range of solid materials. However, for many nuclei acquiring data is often time consuming either due to the long relaxation delays required to obtain quantitative data, low abundance of NMR active nuclei, or limited sample amounts. Intense research has been focused on methods that can reduce the time required to obtain solid-state NMR spectra. Of these, dynamic nuclear polarization (DNP) is a rapidly expanding area of research in solid-state NMR and in favourable cases enhancements can exceed hundreds of times that of standard NMR methods. Much work in this field has been focused on mesoporous silica due to both the challenges inherent with ^{29}Si NMR, and the role these materials play in catalysis and separations technologies[1-4]. These DNP methods have shown great promise for characterizing these materials and have been shown to specifically probe the chemically active surface[5-8]. However, DNP NMR typically requires expensive magnet and probe upgrades. Despite advances in commercialization, DNP is far from being standard methodology in most chemistry labs. Further, most methods also require the addition of radical containing solutions that may render precious samples useless for future chemistry experiments and may alter the chemistry at the surface. Much of our previous work on silica materials has focused on the chemical reactions that occur at these surfaces, and reaction with radicals could eliminate many of these signatures[9-14]. Further, such treatment may not be feasible in instances where the samples are acutely toxic, reactive, or radioactive.

The addition of Carr-Purcell-Meiboom-Gill (CPMG) during the acquisition of solid-state NMR experiments can significantly reduce the time to acquire these data. The CPMG-type acquisition collects the data as a refocused echo train that resamples the NMR free-induction decay (FID) numerous times during acquisition. By adjusting the number of echoes and their resampling frequency, a dramatic increase in the amount of signal that can be acquired during a solid-state NMR experiment can be obtained. The CPMG acquisition is beneficial since it is only a data collection procedure and requires no pre-processing of the material. This procedure, however, does have some significant limitations. The largest limitation is that the signal decays during the CPMG acquisition via transverse relaxation (T_2), so signals with longer relaxation rates will be represented disproportionately compared to those with fast rates. Therefore, quantitative information about the relative populations often cannot be adequately obtained with standard processing methods. Advanced processing methods have been identified to ameliorate these issues and can provide additional signal to noise enhancements. However, these methods often require complex modelling of the FID's to achieve these results[15-19]. In amorphous systems or systems where the spin states are unknown such modelling is difficult.

Our group has been exploring the use of chemometric methods for the model-free analysis of solid-state NMR data[9, 13]. In the basic two-dimensional application, these methods identify spectral components that vary as a function of an

[a] Physical and Life Science Directorate, Lawrence Livermore National Laboratory, Livermore, CA, USA
[b] Systems Research and Analysis, Sandia National Laboratories, Livermore, CA, USA
[c] Department of Chemistry, Hunter College of City University of New York, New York, NY, USA
See DOI: 10.1039/x0xx00000x

This journal is © The Royal Society of Chemistry 20xx

Please do not adjust margins

independent variable. In the instance of cross-polarization magic angle spinning (CP/MAS) experiments, the easiest parameter to vary is the CP contact time, but any independently varied parameter that changes the spectral features such as pulse delay or rotor period could be used. In the above studies, we could differentiate between the direct protonated silanol surface environment on the amorphous silica surface from that of deprotonated silanol and siloxane sites that were observed through ^{1}H spin diffusion and identify the binding sites for paramagnetic metal species[9, 13]. Similar methods have also been utilized to extract unique and complex ^{27}Al spectral components that were observed to change as a function of synthesis conditions in silicate minerals[20]. Beyond the choice of the number of components to use in the fitting procedure, these methods are model-free and can be used to fit complex spectral lineshapes in the absence of a model for their dynamics. Other methods such as CORE and SCORE all depend on initial models of the spectral dynamics and use brute force fitting of the data matrix to obtain unique spectral features[21-25]. These methods are commonly implemented in solution NMR studies and provide large increase in sensitivity and resolution. In this submission, we exploit the nature of the CPMG type acquisition that allows us to transform an initial two-dimensional data set into a data dense three-dimensional data set. This data set is subsequently used in a tensor-rank decomposition to extract the independently varying spectral components. The method extracts important spectral dynamics in addition to reduction in noise from the data sets. These methods reveal valuable information about the surface chemistry of mesoporous functionalized silica materials.

2. Methods

2.1 Materials

The samples studied here were organically-modified mesoporous silica (SBA-15 type) materials. Spherical SBA-15 mesoporous silica particles were synthesized using a hydrothermal synthetic method adapted from Katiyar *et al*[26]. Particle synthesis involved combination of a triblock copolymer (polyethylene glycol-polypropylene glycol-polyethylene glycol) with hexadecyl trimethylammonium bromide and trimethyl benzene in a weight ratio of 5:1:1.5 as structure directing agents in a mixture of 1.5 M HCl and ethanol heated to 35 °C. After obtaining homogeneity, tetraethyl orthosilicate was added and the solution heated to 80°C for 5 hours under static conditions, followed by heating in an oven at 120 °C. Particles were filtered and calcined at 550 °C for six hours. The mesoporous silica surface was functionalized post-synthesis using a surface polymerization method developed by Sander and Wise.[27] After drying the silica under vacuum overnight, it was suspended in toluene and water was added stoichiometrically to achieve a surface coverage of 10 H_2O molecules per square nanometer of silica surface. Ligands containing reactive ethoxysilane anchors were then added in a ratio of 6.25 molecules per square nanometer, and the solution refluxed for six hours followed by distillation to 110 °C to encourage further condensation of silane groups onto the surface. Functionalized particles were washed with toluene and isopropanol and stored in an evacuated desiccator. Two different types of organic ligand were used: a phosphonate, diethylphosphatoethyl triethoxysilane (DPTS) from Gelest, and a diglycolamide (DGA), a 4:1 mixture of N,N-(dipropyl)-N'(methyl),N'(3-[trimethoxysilyl]propyl)-3-oxapentane diamide and N,N-(dipropyl)-N'(methyl),N'(3-[monoethoxydimethoxysilyl]propyl)-3-oxapentane diamide from Technocomm, Ltd.

2.2 NMR Measurements

The $^{29}Si\{^{1}H\}$ cross-polarization magic angle spinning (CP/MAS) spectra of the DPTS sample were collected at a spinning rate of 10 kHz on a 300 MHz TecMag Apollo console using a Bruker XY probe configured for 4 mm (o.d.) rotors. A variable contact time experiment was run by collecting spectra at 15 different contact times ranging from 0.5 to 15 ms using a CPMG type acquisition where a total of 100 echoes were collected at an echo spacing of 6 ms. A 10.5 µs excitation pulse was applied to the proton channel ($\nu_{rf,H}$ = 24 kHz). The same r.f. power was used for the ^{1}H contact pulse. The ^{29}Si contact pulse was matched at $\nu_{rf,Si}$ = 15 kHz and a 18 µs inversion pulse ($\nu_{rf,Si}$ = 28 kHz) was used for ^{29}Si in the CPMG train. The echo spacing was chosen such that the full echo was collected. Continuous wave ^{1}H decoupling ($\nu_{rf,H}$ = 42 kHz) was applied during acquisition of the echoes. Additionally, $^{29}Si\{^{1}H\}$ CP/MAS spectral sets for the DGA sample were collected using a Revolution NMR HX probe configured for 4 mm (o.d.) rotors on a 400 MHz Bruker Avance spectrometer using the same contact times, CPMG delays and number echoes used on the Apollo spectrometer. A 6.5 µs excitation pulse was applied to the proton channel ($\nu_{rf,H}$ = 38 kHz). The same r.f. power was used for the ^{1}H contact pulse and decoupling during echo acquisitions. The ^{29}Si contact pulse was matched at $\nu_{rf,Si}$ = 19 kHz and 12 µs inversion pulse was used for ^{29}Si in the CPMG train ($\nu_{rf,Si}$ = 42 kHz). All ^{29}Si spectra were referenced with respect to tetramethylsilane (TMS) using a sample of the mineral kaolinite as an external chemical shift reference set to -92 ppm.

2.3 Data Processing

All data analyses were performed using custom written Python scripts. A sample data set collected on the Bruker Avance and a sample Python script are provided in the supporting information. Prior to analysis, the full complex CPMG free-induction decays (FID) were split into individual echoes using the echo spacing defined in the pulse sequence. The real and imaginary data were interleaved resulting in a single real valued data set. This interleaved data was used to construct the full 3D data matrix used in the tensor-rank decomposition. A tensor-rank decomposition is like 2D matrix decomposition but generalized to higher dimensional data sets. In our case of a rank-three tensor ($\boldsymbol{\chi}$), the tensor rank decomposition finds the solution such that the tensor can be approximated by the sum of **R** outer products of three vectors **a**, **b**, and **c** with lengths equivalent to that of each of the three dimensions.

This journal is © The Royal Society of Chemistry 20xx

Please do not adjust margins

$$\chi \approx \sum_{r=1}^{R} a_r \circ b_r \circ c_r$$

(1)

A review of tensor decomposition methods is given in Kolda and Bader.[28] A tensor-rank decomposition of the full 3D data set analysis was performed using the cp_als implementation included in the scikit-tensor Python package.[29] The model was initialized using high-order singular value decomposition (HOSVD) rather than a random 3D matrix. The random matrix resulted in results that were not reproducible. This implementation of the tensor-rank decomposition requires a user determined choice of the number of components to be used in the fitting. The final number of components used to reconstruct the data was determined by increasing the number of components until one that represents majority noise is included in the result. For the CP/MAS data sets, the number of components needed was two. After analysis, the extracted FID's were recast into complex data sets, the echoes zero-filled evenly both forward and back, apodized using a sinebell function, and Fourier transformed. To adjust for the loss of signal due to T_2 relaxation, the signals were scaled according to extrapolations to zero time using least squares fitting of the T_2 data to a single exponential decay. Phasing was accomplished by performing a magnitude transform on the spectral data. The loss in resolution due to the magnitude transform was negligible for the samples studied. The CP kinetics information was obtained by fitting the intensity variation as a function of contact time using a classical CP kinetics equation.[30]

2.4 Error Analysis

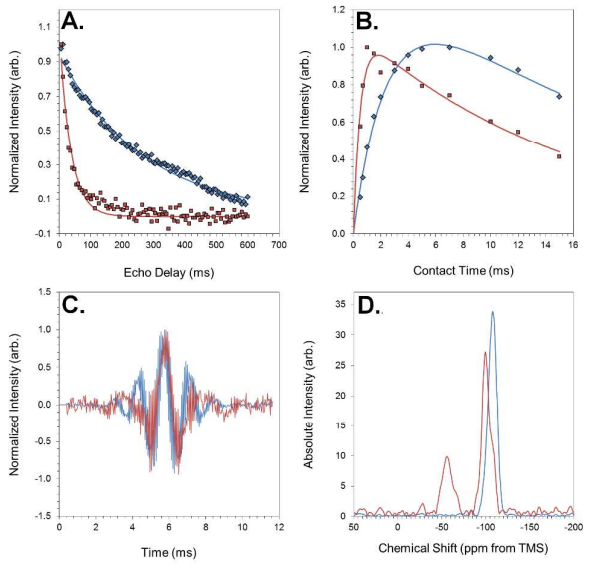

Fig. 1 Data derived from the tensor-rank decomposition of variable contact time $^{29}Si\{^1H\}$ CP/MAS CPMG NMR data sets for the DPTS-SBA sample. Contributions from component 1 are given in blue and those from component 2 are given in red (a) The extracted T_2 data points (solid symbols) and their corresponding least-square fits (solid lines). (b) The extracted variable contact time data points (solid symbols) and their corresponding least squares fits to standard CP kinetics equation (solid lines). (c) Extracted FID's presented in real space as alternating real and imaginary data points. (d). Full echo Fourier transforms of the FID's presented in (c) and corrected for difference in magnitude using the T_2 fits in (a)

To assess the ability of the method to accurately reconstruct the true peak shapes, positions, and intensity variation as a function of contact time (CP kinetics), a best fit to the reconstructed data was obtained by deconvolving the reconstructed data obtained at a 3 ms contact time using a sum of pseudo-Voight lineshapes. The data at 3 ms was used since it had the best overall signal to noise for all the observed peaks in the direct CP data. The positions and widths of the peaks were then fixed for subsequent fits of the direct CP collected data and the comparison spectra obtained from the CPMG reconstruction. Only the peak amplitudes could vary.

Table 1. Best fit parameters and peak assignment for the deconvolution of the two components extracted from the tensor-rank decomposition. Component 1 and 2 are those represented by red and blue in Figure 1, respectively. Errors provided on the direct fits to the data.

Peak assignment	T^1	T^2	T^3	Q^2	Q^3	Q^4
Comp. 1						
Relative intensity (%)	1.8 ±0.6	24.5 ±0.3	2.9 ±0.3	1.0 ±0.2	57.0 ±0.3	12.7 ±0.
Position (ppm)	-48.7 ±0.4	-56.1 ±0.2	-66.4 ±0.3	-89.8 ±0.2	-99.6 ±0.1	-108.4 ±0.1
Width (ppm)	4.7 ±0.9	10.7 ±0.7	5.4 ±0.7	3.0 ±0.6	8.7 ±0.1	6.0 ±0.2
Comp. 2						
Relative intensity (%)	-	-	-	-	52.5 ±7.5	47.5 ±7.5
Position (ppm)	-	-	-	-	-105.2 ±0.6	-109.6 ±0.2
Width (ppm)	-	-	-	-	10.7 ±0.3	8.5 ±0.3

The error bars on the integrated intensities were assessed by using a Monte Carlo error estimation method. This method was chosen since the uncertainties in the NMR deconvolutions are low and depend heavily on values that were fixed by the user. By allowing these values to vary at random, a truer estimate of the fitting uncertainty can be obtained. A similar procedure was used to estimate the uncertainty in fits of chemical shift anisotropy (CSA).[31] The procedure uses the best fit parameters for each of the data sets as a starting point. The difference between the best fit widths and positions for the direct CP and reconstructed CPMG spectra were first obtained. These differences were used as boundary conditions within which the peak widths and positions for each of the 6 peaks could be randomly assigned for subsequent fits to each of the 4 spectra in both the direct CP and reconstructed CPMG data sets. Further, the percent Gaussian characteristic of each peak was also allowed to randomly vary between 0 and 100 % since the choice of peak shape typically was left to user choice. This procedure was repeated 10 000 times for both the data sets and the errors were obtained as the standard deviation of the integrated intensities obtained from each fit.

3. Results and Discussion

The basic procedure is illustrated with a variable contact time (VCT) $^{29}Si\{^1H\}$ CP/MAS data collected for a DPTS functionalized mesoporous silica (Figure 1). All experimental data for this sample were collected on 10 mg of sample contained in an

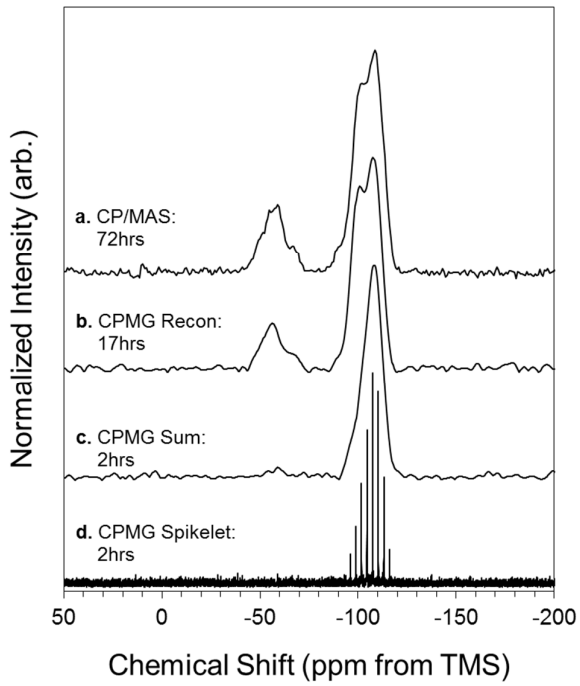

Fig. 2 A comparison of $^{29}Si\{^{1}H\}$ CP/MAS data collected at 10 kHz using a 3 ms contact time for a DPTS-SBA sample. Time needed to collect each spectrum is given for each (a) Standard $^{29}Si\{^{1}H\}$ CP/MAS NMR spectrum. (b) Spectrum for the reconstructed using the reconstruction method described in the text. (c) Data reconstructed by summing the individual CPMG echoes prior to Fourier transform. (d) A Fourier transform of the full CPMG echo train to produce a "spikelet" spectrum.

insert within a 4 mm (o.d.) rotor and due to the limited sample amount, it required more time for standard acquisitions on a full rotor. The data is collected using a CPMG-type acquisition where 100 echoes were collected. The three axes of variation represent the T_2 decay (Figure 1a), the intensity variation as a function of contact time (Figure 1b), and the FID's (Figure 1c) of the two components identified by this method. The Fourier transformed spectral components are presented in (Figure 1d). The two components illustrate very different T_2 values and CP kinetics behaviour. The first component (red in Figure 1) can be fit with 6 peaks (Table 1) and has a shorter T_2 (T_2 = 36.3 ms) and more rapid CP kinetics (T_{SiH} = 0.5 ms, $T_{1\rho,H}$ = 16.3 ms). The second (blue in Figure 1) contains only two peaks (Table 1) and has a longer T_2 of 274 ms and slower CP kinetics (T_{SiH} = 2.4 ms, $T_{1\rho,H}$ = 22.2 ms).

The method can also be used to reconstruct any spectrum along the VCT curve. For this reconstruction, the spectral components are first adjusted for T_2 decay by fitting their T_2 decays and back calculating their initial intensity at zero time. The second step is to multiply these T_2 scaled components by their relative intensities at a given contact time and co-add them to obtain the final reconstructed spectrum. In Figure 2 we compare a standard CP/MAS spectrum collected for the DPTS functionalized SBA sample (Figure 2a) to that reconstructed from the CPMG data at the same 3 ms contact time (Figure 2b). The results show good agreement in terms of their peak positions, widths, and intensities (Table 2). Additionally, we can compare the results of our new method (Figure 2b) to the standard processing methods used for CPMG data sets. The standard methods either stack and sum each echo (Figure 2c), or perform a Fourier transform (FT) on the full echo train (Figure 2d). The later produces a spectrum containing a "spikelet" of peaks that map out the spectral lineshape. In both reconstructions, little to no intensity exists in the -40 to -60 ppm range. These results illustrate the major

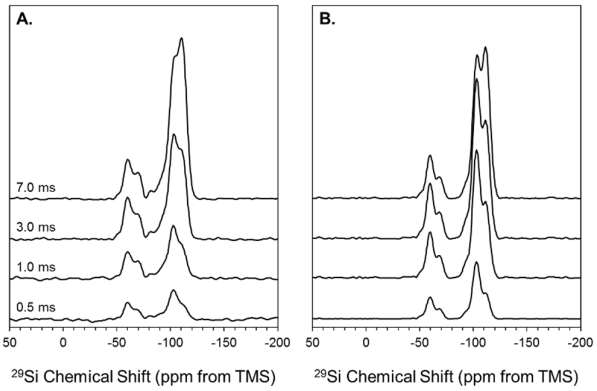

Fig. 3 A comparison of $^{29}Si\{^{1}H\}$ CP/MAS data collected for a DGA functionalized silica **A.** at four different contact times compared to **B.** spectra reconstructed from a VCT CPMG data set.

CPMG						
Relative intensity (%)	0.4 ±0.1	15.3 ±0.1	8.0 ±0.1	8.7 ±0.1	40.2 ±0.1	27.4 ±0.1
Position (ppm)	-50.0 ±0.1	-58.6 ±0.1	-67.8 ±0.1	-91.9 ±0.1	-102.0 ±0.1	-111.1 ±0.1
Width (ppm)	3.5 ±0.1	7.4 ±0.1	6.0±0.1	6.7 ±0.1	8.1 ±0.1	7.7 ±0.1

fundamental issue with the CPMG type acquisition. Above we observed that one spectral component has a much longer T_2 decay than the other. Therefore, the component with the longer T_2 decay is disproportionately represented in the transformed data of the full echo train. These issues illustrate the biggest detriment of the CPMG acquisition, which is that the resulting intensities are not representative of the true species distribution.

In addition to reproducing the results of standard CP/MAS, our new processing procedure provides a dramatic increase in time savings. The $^{29}Si\{^{1}H\}$ CP/MAS spectrum in Figure 2a required 72 hrs of active acquisition time due to the limited amount of sample available for analysis. The full VCT $^{29}Si\{^{1}H\}$ CP/CPMG data set used in the reconstruction required 17 hrs of active acquisition in comparison. We have estimated the time it would take to collect a VCT $^{29}Si\{^{1}H\}$ CP/MAS dataset of comparable quality by measuring the signal to noise per acquisition of the most intense peak in the 3 ms data sets at -111 ppm. The amplitude of the noise was taken as the average intensity over the interval of 100 to 0 ppm where no peaks are observed. The signal to noise measured is 98 and

This journal is © The Royal Society of Chemistry 20xx

Please do not adjust margins

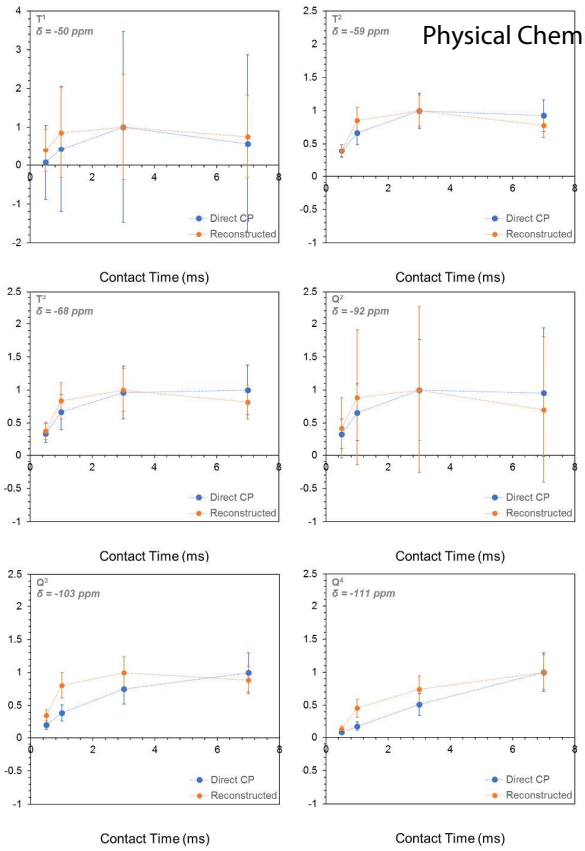

Fig. 4 Comparison of the normalized CP kinetics curves for the DGA sample for each of the six peaks at the given chemical shift collected using direct CP measurements (blue) and using the reconstruction method (orange). The intensities in each panel are normalized such that the maximum intensity for each peak over the VCT series is 1. Error bars represent the error in intensity as described in the text.

118 for the traditionally collected and reconstructed spectra, respectively. Since the traditional spectra required 12 9868 scans at a 2 s pulse delay, a comparable spectrum would require 105.23 hrs of acquisition time. Assuming comparable time to collect each of the 12 VCT spectra a full VCT curve for this sample would require 52.6 days of acquisition time. This estimate of course neglects that spectra collected at different contact times will have major differences in peak intensities and may require longer acquisitions to resolve minor peaks. However, it is clear based on this rough estimate that a dramatic times savings is realized with the CPMG reconstruction method.

Given the above analysis, a full data VCT $^{29}Si\{^{1}H\}$ CP/MAS data set for the DPTS sample would have taken prohibitively long time to acquire. Therefore, we collected a set of spectra at contact times 0.5, 1.0, 3.0, and 7.0 ms collected using traditional CP/MAS acquisition on a digylcolamide (DGA) functionalized material where a larger sample amount could be used. This data was compared to reconstructed data from the CPMG data set and used to assess the ability of the reconstruction method to accurately reproduce the spectra at differing contact times. Comparison of the standard CP spectra (Figure 3A) to the reconstructed spectra (Figure 3B) do show some amplitude differences between the two sets of data. However, the peak widths and positions as well as the CP kinetics are accurately reproduced by the CPMG reconstruction and are within the estimate error of the measurements (Table 2 and Figure 4). The amplitude differences are probably due to the long interpulse delays (6 ms) used to collect the full echoes during the CPMG acquisition. Therefore, the faster relaxing components may be experiencing greater amplitude uncertainties due to the need to back calculate the initial intensities from the T_2 data.

The data extracted from this method also provide valuable insight into the structure and chemistry of these materials. Beyond the dramatic increase in signal to noise, the biggest benefit is derived by the co-collection of both T_2 and CP-kinetics. In this case, the two components shown in Figure 1d can be assigned to two distinct protonation environments within these materials. The first component is represented by long relative T_2, and slow CP kinetics (Figure 2 blue). Combined with the spectral component containing mostly Q^4 siloxane peaks (-110 ppm) we can assign this environment to bulk silica that is close enough to the surface to CP through spin diffusion to the proton spin bath. The second component, therefore, represents the direct surface environment of the functionalized mesoporous silica. This assignment is consistent with both the relatively short T_2, rapid CP kinetics, and the appearance of peaks from silanols (-90 to -106 ppm) and the functionalized surface sites (-50 to -70 ppm)[10-12]. The presence of protons on the surface mediates both the short T_2 relaxation and the rapid CP kinetics of these surface sites. The non-unique CP behaviour of the silica sites is likely resultant from rapid ^{1}H spin diffusion. These same environments are derived in all the functionalized SBA samples we have studied and illustrates that the method provides powerful information about the direct surface environments of these materials.

4. Conclusions

The methods presented here show a dramatic time savings for the collection of data rich NMR spectral sets using conventional NMR pulse sequences and equipment. Further, the data processing method can be applied to a wide range of data where one independent variable is changed over the course of the experiment. It should be noted that these methods thus far have only been developed for data sets where the three dimensions are not correlated and orthogonal to one another. The application of such methods to data sets where the spectra encounter changes in chemical shift or phase would be desirable but still are outside of the scope for the proposed data processing methods. Since this is a data processing method, these methods could be applied in conjunction with other echo acquisition methods such as PIETA that have been shown to have an advantage over CPMG acquisition schemes[32] or signal enhancement protocols such as DNP to allow for unprecedented signal enhancement. Further, this method is model free and requires no a-priori knowledge about the samples or the spins systems. Therefore, it could be easily applied to systems containing quadrupoles, complex dynamics, or exchange that produce complex overlapping spectral lineshapes.

This journal is © The Royal Society of Chemistry 20xx

Please do not adjust margins

Conflicts of interest

There are no conflicts to declare.

5. Acknowledgements

This work was supported by the Subsurface Biogeochemical Research Program of the U.S. Department of Energy's Office of Biological and Environmental Research. This paper describes objective technical results and analysis. Any subjective views or opinions that might be expressed in the paper do not necessarily represent the views of the U.S. Department of Energy or the United States Government. This document was prepared as an account of work sponsored by an agency of the United States government. Sandia National Laboratories is a multimission laboratory managed and operated by National Technology & Engineering Solutions of Sandia, LLC, a wholly owned subsidiary of Honeywell International Inc., for the U.S. Department of Energy's National Nuclear Security Administration under contract DE-NA0003525. Neither the United States Government nor Lawrence Livermore National Security, LLC, nor any of their employees makes any warranty, expressed or implied, or assumes any legal liability or responsibility for the accuracy, completeness, or usefulness of any information, apparatus, product, or process disclosed, or represents that its use would not infringe privately owned rights. Reference herein to any specific commercial product, process, or service by trade name, trademark, manufacturer, or otherwise does not necessarily constitute or imply its endorsement, recommendation, or favoring by the United States government or Lawrence Livermore National Security, LLC. The views and opinions of authors expressed herein do not necessarily state or reflect those of the United States government or Lawrence Livermore National Security, LLC, and shall not be used for advertising or product endorsement purposes. Prepared by LLNL under contract DE-AC52-07NA27344.

6. Notes and references

1. T. Kobayashi, D. Singappuli-Arachchige, Z. Wang, I. I. Slowing and M. Pruski, *Physical Chemistry Chemical Physics*, 2016, **19**, 1781-1789.
2. O. Lafon, A. S. L. Thankamony, T. Kobayashi, D. Carnevale, V. Vitzthum, I. I. Slowing, K. Kandel, H. Vezin, J.-P. Amoureux, G. Bodenhausen and M. Pruski, *Journal of Physical Chemistry C*, 2013, **117**, 1375–1382.
3. T. Kobayashi, O. Lafon, A. S. L. Thankamony, I. I. Slowing, K. Kandel, D. Carnevale, V. Vitzthum, H. Vezin, J.-P. Amoureux, G. Bodenhausen and M. Pruski, *Physical Chemistry Chemical Physics*, 2013, **15**, 5553-5562.
4. A. J. Rossini, A. Zagdoun, M. Lelli, D. Gajan, F. Rascon, M. Rosay, W. E. Maas, C. Coperet, A. Lesage and L. Emsley, *Chemical Science*, 2012, **3**, 108-115.
5. M. A. Hope, D. M. Halat, P. C. M. M. Magusin, S. Paul, L. Peng and C. P. Grey, *Chemical Communications*, 2017, **53**, 2142-2145.
6. A. J. Rossini, A. Zagdoun, M. Lelli, A. Lesage, C. Copéret and L. Emsley, *Accounts of Chemical Research*, 2013, **46**, 1942-1951.
7. F. A. Perras, T. Kobayashi and M. Pruski, *Journal of the American Chemical Society*, 2015, **137**, 8336–8339.
8. A. Lund, M. F. Hsieh, T. A. Siaw and S. I. Han, *Physical Chemistry Chemical Physics*, 2015, **17**, 25449-25454.
9. H. E. Mason, S. J. Harley, R. S. Maxwell and S. A. Carroll, *Environmental Science & Technology*, 2012, **46**, 2806-2812.
10. J. A. Shusterman, H. E. Mason, J. Bowers, A. Bruchet, E. C. Uribe, A. B. Kersting and H. Nitsche, *Acs Applied Materials & Interfaces*, 2015, **7**, 20591-20599.
11. E. C. Uribe, H. E. Mason, J. A. Shusterman, A. Bruchet and H. Nitsche, 2016, **45**, 10447-10458.
12. J. Shusterman, H. Mason, A. Bruchet, M. Zavarin, A. B. Kersting and H. Nitsche, *Dalton Transactions*, 2014, **43**, 16649-16658.
13. H. E. Mason, J. D. Begg, R. S. Maxwell, A. B. Kersting and M. Zavarin, *Environmental Science: Processes and Impacts*, 2016, **18**, 802-809.
14. E. C. Uribe, H. E. Mason, J. A. Shusterman and W. W. Lukens, *Dalton Transactions*, 2017, **46**, 544-5456.
15. Y. G. Kolyagin, A. V. Yakimov, S. Tolborg, P. N. R. Vennestrøm and I. I. Ivanova, *Journal of Physical Chemistry Letters*, 2016, **7**, 1249–1253.
16. F. H. Larsen, H. J. Jakobsen, P. D. Ellis and N. C. Nielsen, *Journal of Physical Chemistry A*, 1997, **101**, 8597–8606.
17. F. H. Larsen and I. Farnan, *Chemical Physics Letters*, 2002, **357**, 403–408.
18. J. W. Wiench, V. S.-Y. Lin and M. Pruski, *Journal of Magnetic Resonance*, 2008, **193**, 233–242.
19. A. V. Yakimov, Y. G. Kolyagin, S. Tolborg, P. N. R. Vennestrøm and I. I. I., *Journal of Physical Chemistry C*, 2016, **120**, 28083–28092.
20. R. J. McCarty and J. F. Stebbins, *American Mineralogist*, 2018, **102**, 1244-1253.
21. N. Hedin, J. B. S. Ng and P. Stilbs, *Solid State Nuclear Magnetic Resonance*, 2009, **35**, 208-213.
22. M. Nilsson and G. A. Morris, *Analytical Chemistry*, 2008, **80**, 3777-3782.
23. P. Stilbs and K. Paulsen, *Review of Scientific Instruments*, 1996, **67**, 4380-4386.
24. A. A. Colbourne, S. Meier, G. A. Morris and M. Nilsson, *Chemical Communications*, 2013, **49**, 10510-10512.
25. E. L. Lindh, P. Stilbs and I. Furo, *Journal of Magnetic Resonance*, 2016, **268**, 18–24.
26. A. Katiyar, S. Yadav, P. G. Smirniotis and N. G. Pinto, *Journal of Chromotography A*, 2017, **1122**, 13-20.
27. L. C. Sander and S. A. Wise, *Analytical Chemistry*, 1984, **56**, 504-510.
28. T. G. Kolda and B. W. Bader, *SIAM Review*, 2009, **51**, 455-500.
29. M. Nickel, scikit-tensor Library (Version 0.1). Available Online November 2013
30. W. Kolodziejski and J. Klinowski, *Chemical Reviews*, 2002, **102**, 613-628.
31. H. E. Mason, J. J. Hirner, W. Q. Xu, J. B. Parise and B. L. Phillips, *Magnetic Resonance in Chemistry*, 2009, **47**, 1062-1070.

This journal is © The Royal Society of Chemistry 20xx

Please do not adjust margins

32. J. H. Baltisberger, B. J. Walder, E. G. Keeler, D. C. Kaseman, K. J. Sanders and P. J. Grandinetti, *The Journal of Chemical Physics*, 2012, **136**, 211104.

This journal is © The Royal Society of Chemistry 20xx

Please do not adjust margins